EPJ Web of Conferences **40**, 12002 (2013)
DOI: 10.1051/epjconf/20134012002
© Owned by the authors, published by EDP Sciences, 2013

Scaling of Hall coefficient in Co-Bi granular thin films

P. Athanasopoulos[1], C. Christides[1], and Th. Speliotis[2]

[1]School of Engineering, University of Patras, 26504 Rion Patras, Greece
[2]Institute of Materials Science, NCSR Demokritos, 15310 Aghia Paraskevi, Athens, Greece

Abstract. A series of Co-Bi thin films with Co concentrations c=0, 0.05, 0.2, 0.26, 0.3, 0.333, 0.375, 0.545, were grown by magnetron sputtering on Si(100)/SiN_X substrates. Resistivity measurements at zero field (ρ_{xx}) as a function of temperature-T exhibit an exponential variation with T in the region of 240K<T<300K. The Hall coefficient as a function of Co concentration diverges as $\log|c\text{-}0.3|^{0.3}$ for c<0.333, indicating a scaling of R_H nearby a percolation threshold p_c=0.3. Only after proper scaling of the anomalous Hall coefficient R_S the conventional $R_S \propto (\rho_{xx})^n$ dependence can be satisfied.

1 Introduction

In magnetic films the Hall resistivity ρ_H is defined by the phenomenological equation:

$$\rho_H = R_0 B + R_S \mu_o M \tag{1}$$

where **B** is the magnetic induction perpendicular to film surface, R_0 is the ordinary Hall (OH) coefficient, **M** is the magnetization, and R_S is the anomalous Hall (AH) coefficient. Usually, in ferromagnetic metals (FM), R_S satisfies a scaling law [1] with the longitudinal film resistivity ρ_{xx} measured at zero applied magnetic field:

$$R_S = a\rho_{xx} + b\rho_{xx}^2 \tag{2}$$

where the first term is assigned to skew scattering and the second term to side jump mechanism [1]. Generally, three regimes were observed [1] with respect to the dependence of anomalous Hall conductivity (AHC) on the conductivity σ_{xx}. Equation-2 is valid within the metallic regime [1] whereas in the insulating regime other scaling exponents were observed [2]. Bismuth films may exhibit p-type or n-type conduction properties, depending on film texture [3] and the participation of surface states on the different crystallographic faces [4]. In our study Cobalt (FM) and semimetal Bismuth layered thin film structures are used to investigate the effect of FM/semimetal junctions in Hall resistivity measurements.

2 Experimental Details

A series of thin film Co/Bi structures were grown by magnetron sputtering on Si(100)/SiN_X substrates with rectangular shapes of 5x5mm^2, using a base pressure of Ar-gas about 10^{-8} Torr, without to control the substrate temperature during film deposition. Specifically, the sample compositions are: two pure Bi films with 15nm and 50nm thicknesses, denoted as Bi(15nm) and Bi(50nm), two trilayer structures of Bi(10nm)/Co(1nm)/Bi(10nm), and Bi(10nm)/Co(5nm)/Bi(10nm), one bilayer structure of Bi(10nm)/Co(5nm), and four multilayer structures with each one composed by ten repetitions of the same [Bi/Co] bilayer unit, denoted as $[\mathrm{Bi(0.7nm)/Co(2nm)}]_{10}$, $[\mathrm{Bi(1nm)/Co(2.4nm)}]_{10}$, $[\mathrm{Bi(2.4nm)/Co(4nm)}]_{10}$, and $[\mathrm{Bi(2.4nm)/Co(4nm)}]_{10}$. The nominal thickness values of Co and Bi layers were reduced to Co concentrations, c-Co, (0, 0.05, 0.2, 0.26, 0.3, 0.333, 0.375, 0.545) by dividing the subtotal of Co layer thickness with total film thickness. The results in Fig.2 are tabulated with increasing order of c-Co.

Resistivity and magneto-transport measurements were performed on the as-made films with a PPMS, using the Van der Pauw method in magnetic fields up to B=9T perpendicular to film-plane. All raw data collected from Hall resistance measurements were corrected according to Ref.[5] to obtain the final loops of ρ_H vs B and Hall coefficient R_H vs B shown in Figs.1, 2. X-ray diffraction (XRD) measurements reveal that all films are polycrystalline. Specifically, the predominant Bragg-peaks with (00*l*) indices (*l*=3, 6), observed in pure Bi films, decrease towards to zero intensity as c increases, indicating a progressive change in texture of Bi layers with c-Co.

3 Results

Fig.1a shows representative ρ_H vs B data and isothermal magnetization M vs B loops observed in Co-rich film at 5K. Fig.1b shows three selected M vs B loops at 5K that span the c-Co range, indicating that the saturation magnetization M_S values are strongly affected by c-Co

This is an Open Access article distributed under the terms of the Creative Commons Attribution License 2.0, which permits unrestricted use, distribution, and reproduction in any medium, provided the original work is properly cited.

Article available at http://www.epj-conferences.org or http://dx.doi.org/10.1051/epjconf/20134012002

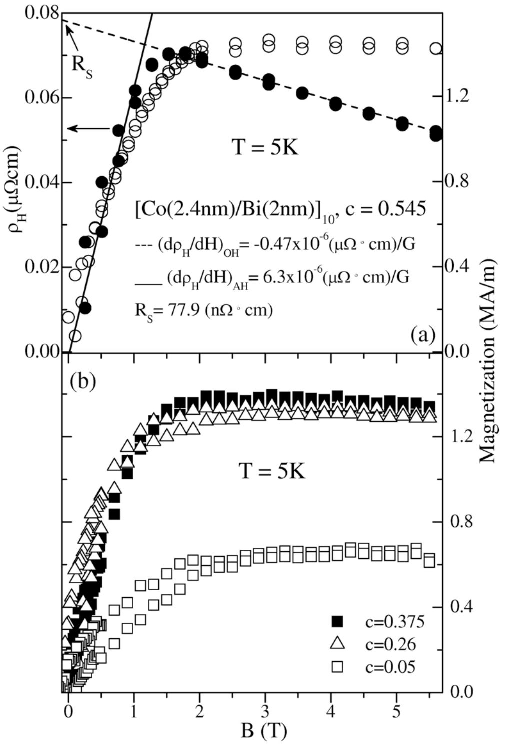

Fig.1. (a) Indicative Hall resistivity ρ_H (•) and magnetization-M (o) loops that explain the estimation of R_0 from the high-field slope and R_S from the point of intersection with ρ_H-axis. (b) Selected isothermal magnetization loops, showing that saturation of magnetization M_S occurs at $B_S \approx 2T$ for T=5K.

whereas the saturation field B_S (and thus magnetic anisotropy) are not influenced by c-Co at a fixed temperature. Thus, the non linear dependence of the Hall coefficient $R_H=\rho_H/B$ on B, observed in Fig.2, cannot be attributed to magnetization effects above 2T. In addition, Fig.2a shows that pure Bi film exhibits non linear R_H vs B curves above 2 Tesla for T≤100K. As we show in a forthcoming publication, these results cannot be fitted with equations used in the two-band model. The observed R_H vs B curves in Fig.2 can be explained by considering the galvanomagnetic properties of polycrystalline or inhomogeneous metals that depend strongly on the shape and the orientation of the crystallites relative to magnetic field direction [6]. The most important effect of crystalline shape and orientation in these films is the observed change of polarity in R_H vs B loops, from positive to negative in Fig.2, that does not depend on a systematic way from c-Co. As shown in Fig.3, the sign of R_H(8T), which is the value of R_H at 8T in Fig.2, and the sign of R_S, both change from negative to positive as the percentage of preferable orientation of [00*l*]-directions in Bi layers change from perpendicular to parallel in film plane. Note that both, the $R_0=d\rho_H/dH$ and the R_H(8T) values have positive sign in pure Bi films (Fig.3a), indicating that holes are the majority charge carriers [7]. In addition, Fig.3a reveals that R_H(8T) becomes negative in between 0.2<c<0.375, indicating a transition from p-type (holes) to n-type (electrons) majority charge carriers in this region. This transition in R_H(8T) values with c-Co is plotted together with R_0 vs c-Co in Fig.4.

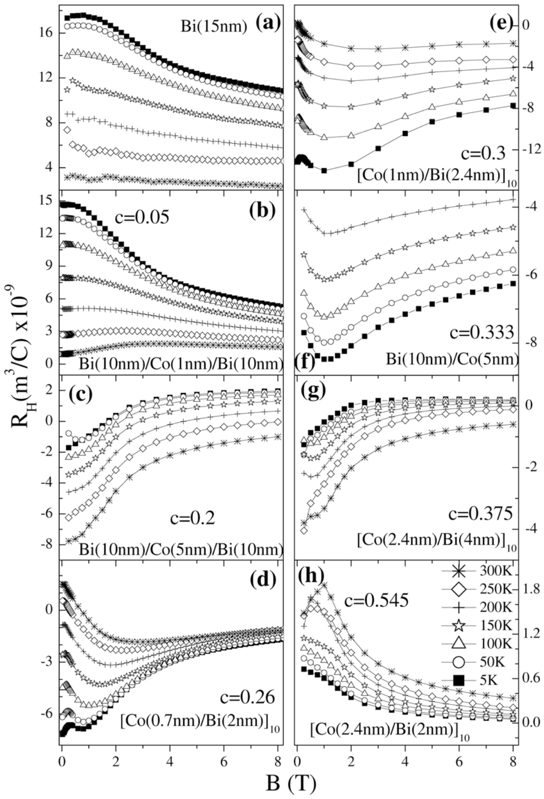

Fig. 2. Hall coefficient R_H vs B curves between 5K and 300K.

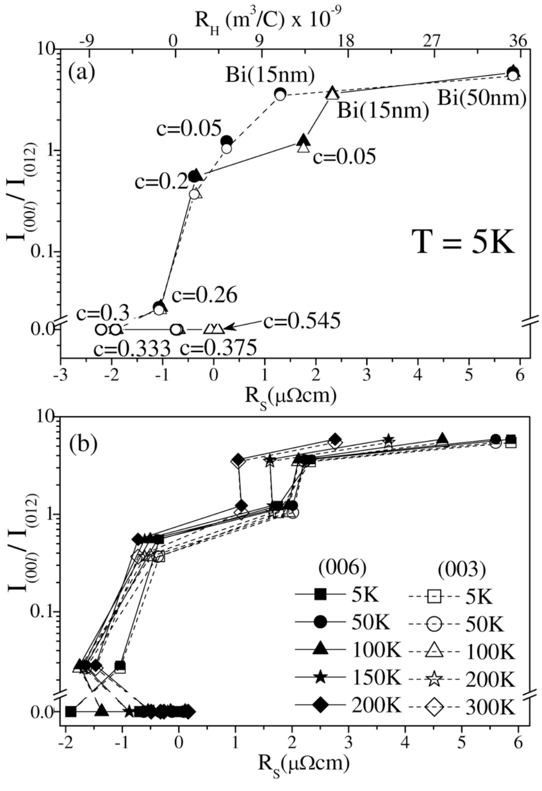

Fig. 3. Semi-log plot of XRD intensities from Bi (00*l*) Bragg peaks (*l*=3 or *l*=6) as a function of: (a) R_H(8T) values (dash line) and R_S values (solid line) at 5K, and (b) R_S values in the range of 5K≤T≤200K. The (003) and (006) indices are plotted with open and dark symbols, respectively. Their intensities were normalized to observed (012) Bragg-peak intensity of Bi.

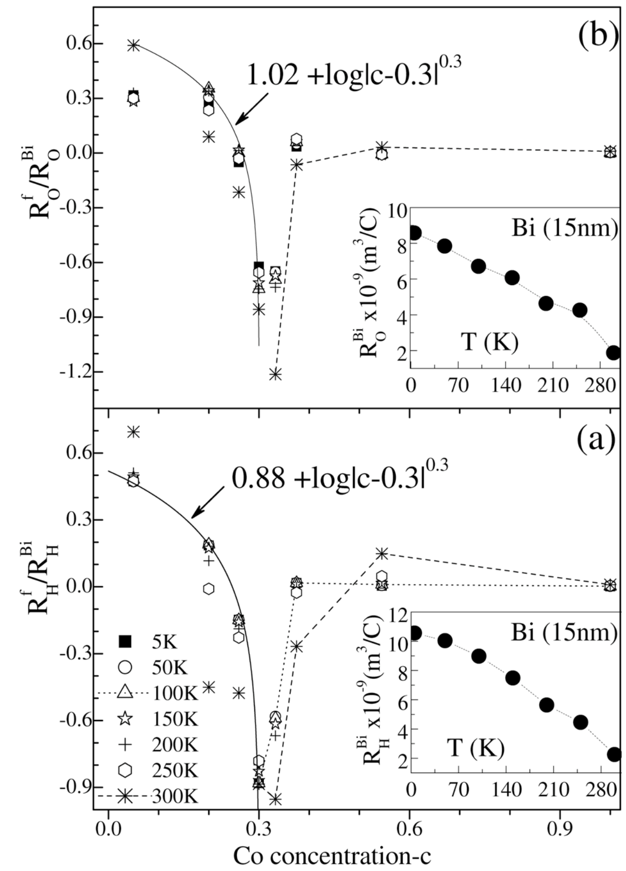

Fig. 4. Scaling of (a) R_H^f and (b) R_0 values with c-Co. Solid lines are fitting curves to equation shown with arrow. Insets show the temperature dependence of R_H^{Bi} and R_0^{Bi} values.

A plot of R_0 values instead of R_H(8T) in Fig.3a will exhibit the same trend, but we plot only the R_H(8T) values for reasons explained below. Fig.3b shows that the sign of R_S does not follow the systematic sign reversal of R_H(8T) or R_0 with c-Co, but depends only on the degree of orientation of [00*l*]-directions in Bi layers relative to film vertical direction. Since Bi exhibits [4] a strong spin-orbit (SO) level splitting along [00*l*]-directions, then Fig.3b may imply that the SO Hamiltonian [8] H_{SO} in Bi is negative for example when [00*l*]-directions are in-plane and positive for out-of-plane, thus, reversing from "*left to right*" direction the effective nonzero transverse electric field created by the SO interaction. In this case a junction with Co may give rise to unequal occupancy of spin-up and spin down states in Co/Bi interfaces. This may contribute a term of *interspin band scattering* [8] to AH effect (AHE), in addition to intrinsic SO coupling term that contributes to AHE with the scattering of itinerant carriers due either to phonons or to thermal spin disorder.

Fig.4a shows normalized Hall coefficient R_H^f values (obtained from Fig.2 at B=8T for every film) to corresponding Bi film values R_H^{Bi} (see the inset) as a function of c-Co. The notation is that superscripts *f* and *Bi* on R_H, R_S and ρ_{xx} parameters indicate that each one is measured on a film of given c-Co≠ 0 and on pure Bi film

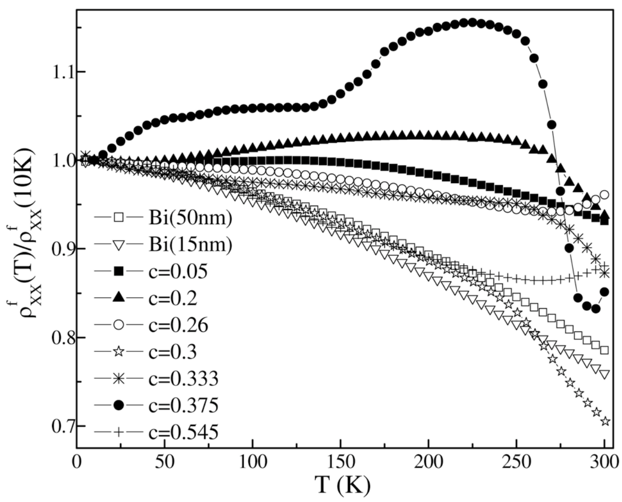

Fig. 5. Temperature dependence of the longitudinal film resistivity ρ_{xx} observed at zero external field in films with different Co concentrations. These ρ_{xx}(T) curves are normalized to the corresponding film ρ_{xx} value observed at T=10K. Lines are guides to the eye.

(c-Co=0), respectively. The R_H^f values were found to diverge as $log|c\text{-}0.3|^{0.3}$ for c<0.333, evidencing a critical behaviour [9] nearby a percolation threshold p_c=0.3, with critical exponent g=0.3. The physical origin of p_c=0.3 might be related to energy balance between the work functions [10] of Co and Bi layers and their Fermi level matching at Co/Bi interfaces, that may create [11] a depletion layer (defining a critical length scale) of hole-like or electron-like carriers in Bi as a function of c-Co. In addition, the same trend of R_H^f vs c-Co appears in all $R_H^f(B)$ values determined for B ≥ 5T. However, a plot of the ordinary Hall coefficient R_0 with c-Co in Fig.4b (determined by the high-field slope in Fig.2, with B>3T) reveals a slightly shifted p_c value at a value of c-Co≈ 0.333. A comparison of c-Co values in Figs.3, 4 and 5(see the inset), where a minimum of *I*(00*l*), R_H^f or R_0, and R_S values occurs, indicates that the p_c value is more likely to be nearby c-Co=0.3. In addition, the same function, $log|c\text{-}0.3|^{0.3}$, fits (solid line) both data sets in Figs.4a and 4b for c-Co≤0.3 in the region of 5K≤T≤250K.

Fig.5 shows the temperature dependence of ρ_{xx} observed in all films at zero applied field. Remarkably, all these films exhibit an exponential variation of ρ_{xx}(T) at 240K<T<300K whereas in some films (c=0.05, 0.2, 0.375) appears a ρ_{xx}≈T^n behavior for T<240K. The exponential dependence in ρ_{xx}(T) curves arises from the dominant contribution of Bi layers to film resistivity, since the observed $\rho_{xx}^{Bi}(T)$ curves of pure Bi films can be simulated with a single exponential function of T in the region of 5K≤T≤300K.

The dominant contribution of $\rho_{xx}^{Bi}(T)$ in the magneto-transport properties of our films can be clearly demonstrated if we try to satisfy Eq.2 for every c-Co by plotting the R_S(T)/ρ_{xx}(T) ratio against the corresponding values of ρ_{xx}(T) from Fig.5. Fig.6 includes two such plots where all parameters are normalized to their values at 5K in order to be able to compare the results for all c-Co values. Fig.6a shows that Eq.2 is not satisfied when the measured value $\rho_{xx}^{f}(T)$ of the corresponding film (in Fig.5) is used, and the inset demonstrates that R_S values as a function of Co concentration at 5K exhibit a minimum at the same p_c=0.3 as the R_H^f in Fig.4a. However, when we keep the actual $R_S(T)$ values for each c-Co and replace the $\rho_{xx}^{f}(T)$ values with the corresponding $\rho_{xx}^{Bi}(T)$ values observed in Bi(15nm) film (from Fig.5) then Fig.6b shows that Eq.2 is satisfied for all the films.

The reason that Eq.2 is satisfied only with $\rho_{xx}^{Bi}(T)$ but is not satisfied with $\rho_{xx}^{f}(T)$, is not clear. Preliminary results from analysis of the experimental data shown in Figs.5 and 6 provide evidence that the conventional scaling of R_S in Eq.2 is maintained by substituting $\rho_{xx}^{Bi}(T)$ because of a proper scaling [12] that involves a critical length scale in Bi side of Bi/Co junctions.

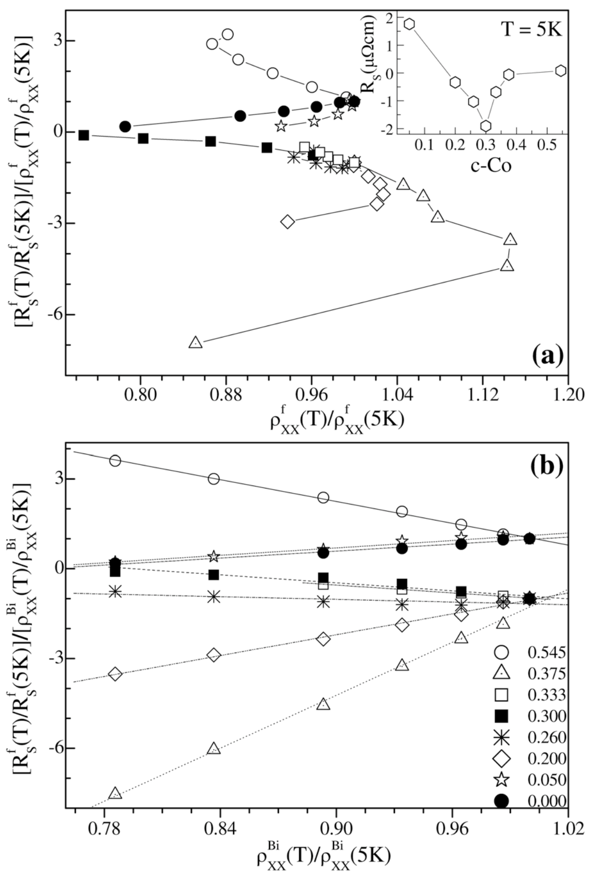

Fig. 6. (a) Normalized AHE coefficients $R_S(T)$ to $R_S(5K)$ of the films are divided by the normalized film resistance at zero field $\rho_{xx}(T)/\rho_{xx}(5K)$, and plotted as a function of $\rho_{xx}(T)/\rho_{xx}(5K)$ of the film. Lines are guides to the eye. The inset shows R_S values at 5K as a function of c-Co. (b) The same $R_S(T)/R_S(5K)$ values divided by the normalized resistance of Bi(15nm) film at zero field, as a function of the temperature dependence of the normalized resistance of Bi(15nm) film. Lines are linear fits satisfying Eq.2. Different symbols correspond to c-Co in different films and are the same in both plots.

4 Conclusion

In summary, magneto-transport measurements in polycrystalline Co/Bi layered thin film structures reveal that R_H^f or R_0 values exhibit (Fig.4) a critical scaling close to a percolation threshold p_c=0.3, with a critical exponent g=0.3. It was observed that between 0.2<c<0.375: (i) both, the OH coefficient R_0 and R_H^f values become negative, evidencing a transition from p-type to n-type majority charge carriers in this region, and (ii) a similar behaviour appears in the plot (Fig.6a, inset) of R_S values as a function of c-Co at 5K. However, the sign of R_S depends on the degree of orientation of [00*l*] crystallographic directions in Bi layers relative to film vertical direction, and is not related with Co concentration. It was shown that the obtained R_S values satisfy Eq.2 only if $\rho_{xx}^{f}(T)$ is replaced by $\rho_{xx}^{Bi}(T)$ values observed in pure Bi(15nm) film. The last two results provide evidence that the dominant contributions to AHE are related with intrinsic and extrinsic mechanisms in Bi side of Bi/Co interfaces.

Acknowledgment

This research has been co-financed by the European Union (European Social Fund – ESF) and Greek national funds through the Operational Program "Education and Lifelong Learning" of the National Strategic Reference Framework (NSRF) - Research Funding Program: Heracleitus II. Investing in knowledge society through the European Social Fund.

References

1. N. Nagaosa, J. Sinova, S. Onoda, A.H. MacDonald, N.P. Ong, Rev. Mod. Phys. **82**, 1539 (2010)
2. X-J. Liu, X. Liu, J. Sinova, Phys. Rev. B **84**, 165304 (2011)
3. K.-S. Wu, M.Y. Chern, J. Appl. Phys. **104**, 033704 (2008)
4. Ph. Hofmann, Prog. Surf. Sci. **81**, 191 (2006)
5. J. Lindemuth, B. Dodrill, IEEE Trans. Magn. **40**, 2191 (2004)
6. D. Stroud and F. P. Pan, Phys. Rev. B **20**, 455 (1979)
7. D. D. Franket and H.T. Chu, Phys. Rev. B **61**, 13183 (2000).
8. C.M. Hurd, *The Hall Effect in Metals and Alloys* (Plenum, New York, 1972), Chap. 5.
9. D. Bergman, Y. Kantor, D. Stroud, I. Webman, Phys. Rev. Lett. **50**, 1512 (1983).
10. J. Buxo, M. Saleh, G. Sarrabayrouse, G. Dorville, J. Berty, M. Brieu, Revue Phys. Appl. **15**, 961 (1980)
11. D. Agassi and T.K. Chu, Apll. Phys. Lett. **51**, 2227 (1987).
12. Y. Tian, L. Ye, X. Jin, Phys. Rev. Lett. **103**, 087206 (2009).